Effect of deflector curvature on hydrodynamic performances of a double-slotted cambered otter-board

Lei WANG[1], *Lu Min WANG*[1], *Jian Gao SHI*[1], *Wen Wen YU*[1], *Guang Rui QI*[1], *Xun ZHANG*[1,*], *Rong Jun ZHANG*[2], and *Tian Shu ZHANG*[2]

[1]Key Laboratory of Oceanic and Polar Fisheries, Ministry of Agriculture; East China Sea Fisheries Research Institute, Chinese Academy of Fishery Sciences, Shanghai 200090, China
[2]China National Fisheries Corporation, Beijing 100032, China

Abstract. The effect of deflector curvature on hydrodynamic performances of a double-slotted cambered otter-board was investigated using engineering models in a wind tunnel. Four different curvature (0.06,0.09, 0.12 and 0.15) were evaluated at a wind speed of 28 m/s. Parameters measured included: drag coefficient C_x, lift coefficient C_y, pitch moment coefficient C_m, center of pressure coefficient C_p , over a range of angle of attack (0° to 70°). These coefficients were used in analyzing the differences in the performance among the four otter-board models. Results showed that the maximum lift coefficient C_y of the otter-board model with the curvature (0.06) of two deflectors was highest (2.020 at α=55°). The maximum C_y/C_x of the otter-board with the curvature (0.12) of two deflectors was highest (3.655 at α=22.5°). A comparative analysis of C_m and C_p showed that the stability of otter-board model with the curvature (0.12) of two deflectors is better in pitch, and the stability of otter-board model with the curvature (0.06) of two deflectors is better in roll. The findings of this study can offer useful reference data for the structural optimization of otter-boards for trawling.

1 Introduction

Otter-boards are an important part of fishing gear for spreading the trawl mouth. The merits of the hydrodynamic performance of otter-boards can be measured on the basis of the lift coefficient of the otter-board, the drag coefficient of the otter-board, and the pitching moment coefficient of the otter-board [1]. Optimizing the structure of otter-boards may improve the hydrodynamic performance of the otter-board [2-3]. Extensive studies on the hydrodynamic performance of otter-boards have been conducted in the United States, Japan, Norway, and other countries [4-8]. In China, researchers have studied the relevant hydrodynamic performance of otter-boards since the early 1980s, including the hydrodynamic performance and optimization of different otter-boards with various structure types [9-13]. Improvements in the hydrodynamic performance of otter-boards has become a major research interest as the development of offshore trawler fleets increasing globally in recent decades. Some studies have shown that the slit in otter-boards can reduce the resistance and improve the stability of otter-boards [14-19]. The following study investigates the importance of the curvature of the deflector within the otter-board. We describe an experiment using otter-board models (n=4 designs) in a wind tunnel in which we measured various hydrodynamic coefficients for a range of angles of attack. The results are relevant as a reference for the study of the structural parameters of the deflector curvature of otter-boards.

2 Material and Methods

2.1 Design and manufacture of otter-board model

The otter-boards evaluated in this study were double-slotted curved structures comprising two deflectors and a main-panel (figure 1). This structure design was based on the used bottom trawl otter-board currently, and was simplified in order to meet objectives and requirements of the study. Only the curvature of two deflectors was modified.

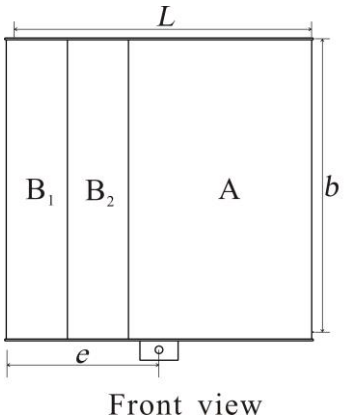

Front view

* Corresponding author: zhangxun007@hotmail.com

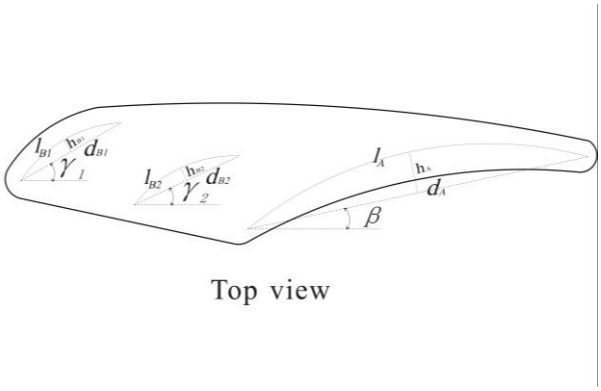

Fig. 1. Structure and parameters of otter-board
Note: L: chord; b: span; e: distance between fulcrum and the front end of model; B_1, B_2: deflector; A: main-panel; γ_1, γ_2: angle of deflector; β: angle of main-panel; l_{B1}, l_{B2}: arc length of deflector; l_A: arc length of main-panel; h_{B1}, h_{B2}, h_A: distance from the vertex of the arc to the arc chord; d_{B1}, d_{B2}, d_A: length of arc chord.

Each of models had an aspect ratio of 1.0, surface area of 0.25 m^2, and were identical in many structural parameters and dimensions (table 1). The curvature of the main-panel was 12% and was consistent in all models. The only parameter that varied between the models was the curvature of two deflectors (δ_{B1}, δ_{B2}). The models are made of steel with painted surfaces (figure 2).

Table 1. Descriptive characteristics of the four model otter boards evaluated in this study.

No.	1	2	3	4
***L*/m**	0.5	0.5	0.5	0.5
***b*/m**	0.5	0.5	0.5	0.5
λ	1	1	1	1
***S*/m²**	0.25	0.25	0.25	0.25
***e*/m**	0.25	0.25	0.25	0.25
γ_1	30°	30°	30°	30°
γ_2	25°	25°	25°	25°
β	6°	6°	6°	6°
l_{B1}	0.127	0.127	0.127	0.127
l_{B2}	0.12	0.12	0.12	0.12
l_A	0.313	0.313	0.313	0.313
δ_{B1}	0.06	0.09	0.12	0.15
δ_{B2}	0.06	0.09	0.12	0.15
δ_A	0.12	0.12	0.12	0.12

Note: *L*: chord; *b*: span; λ (*b*/*L*): aspect ratio; *S* (*L*·*b*): surface area; *e*: distance between fulcrum and the front end of model; γ_1, γ_2: angle of deflector; β: angle of main-panel; l_{B1}, l_{B2}: arc length of deflector; l_A: arc length of main-panel; δ_{B1}(h_{B1}/ d_{B1}), δ_{B2}(h_{B2}/ d_{B2}): curvature of deflector; δ_A(h_A/ d_A) : curvature of main-panel.

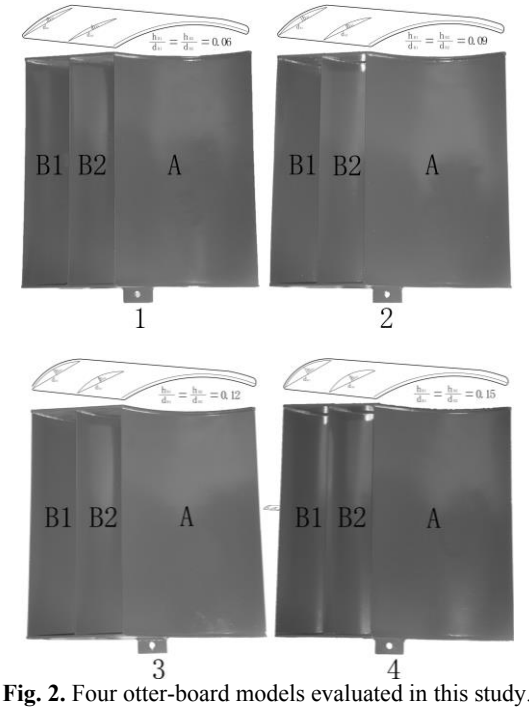

Fig. 2. Four otter-board models evaluated in this study.
Note: A: main-panel; B_1, B_2: deflector.

2.2 Test facility

The wind tunnel used for this experiment was the NH-2 wind tunnel located at Nanjing University of Aeronautics and Astronautics, China. The tunnel is a closed reflux wind tunnel with a double-string test section. The experiment was conducted in a small test section. Dimensions of the test section were 6 m (length) × 3 m (width) × 2.5 m (height). The cross-sectional area was 7.18 m^2. The minimum and maximum wind speeds of the tunnel were 5 m/s and 90 m/s, respectively. Figure 3 illustrates the experimental setup inside the wind tunnel. The otter-board models were attached to a dynamometer compromising a six-component mechanical tower-balance to measure forces in all directions. The data acquisition and processing system used is composed of a pre -amplifier and a four -networked computer system.

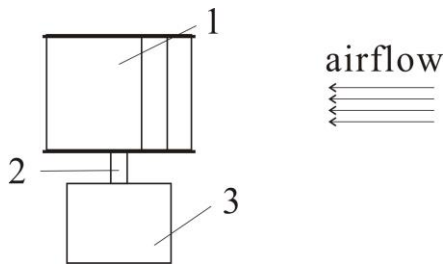

Fig. 3. Installation instruction of otter-board model in wind tunnel.
Note: 1.otter-board model 2.model connection 3.six-component force balance

2.3 Test method

2.3.1 Parameter definition of test model

Test model need to be installed on the wind tunnel in six-component balance mechanical base according to the order, angle of attack of model rotates by the 0 ° -70 ° when the wind speed reaches 28m / s (room temperature 20 ℃),wherein the angle of attack in the range 0 ° -50 °, 2.5 ° intervals to record a measurement data point, after the attack angle 50 °, each measurement interval of 5 ° to record data points, there are 25 sets of data totally, including the drag coefficient C_x, the lift coefficient C_y, the pitch moment coefficient C_m and the center of pressure coefficient C_p.

The relevant parameters of models in the wind tunnel test section are defined as shown in figure 4. In figure 4, O is torque reference point, which is the punch of the model at the bottom. During the test, the resistance of the model is provided by the force of balance along the X-axis direction, the lift is provided by the force of balance along the Z-axis direction, and the pitch moment is provided by the M_y of balance along the Z-axis direction.

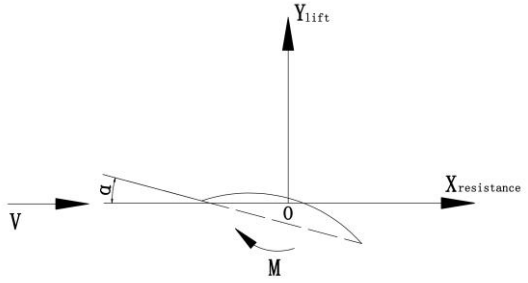

Fig. 4. Parameter definition diagram of test model in wind tunnel.

For this test, Wind speed V=28m/s, when the Reynolds number $R_e=VL/\upsilon=0.93\times10^6$ (coefficient of viscosity $\upsilon=15\times10^6$ m^2·s^{-1}) [14].

2.3.2 Parameter definition of test measurement

Three components: lift Y, drag X, pitching moment M (around the fulcrum), while the distance from the center of pressure to the front-end otter-board $d=e-(M/N)$ [16], (N is the normal force).

Lift coefficient $C_y = \frac{Y}{\rho V^2 S/2}$ [3]; drag coefficient $C_x = \frac{X}{\rho V^2 S/2}$; pitch moment coefficient $C_m = \frac{M}{\rho V^2 SL/2}$; center of pressure coefficient $C_p = \frac{d}{L}$.

Air density ρ=1.225 kg/m^3 in above formula; S is otter-board area (m^2); L is the otter-board chord length (m).

All the experimental data have been carried out the stent disturbance correction which is completed by the method of taking out light pole directly.

3 Results and Discussion

3.1 Drag coefficient and lift coefficient

Data from the experiment included the drag coefficient C_x, the lift coefficient C_y, the pitch moment coefficient C_m, and the center of pressure coefficient C_p. The lift–drag ratio was computed (C_y / C_x), which is an important factor for determining the merits of the hydrodynamic performance of otter-boards. An otter-board with excellent hydrodynamic properties can achieve higher lift–drag ratio and improved stability; such performance can be analyzed by comparing the pitching moment coefficient C_m stencil and the center of pressure coefficient C_p . The test data were divided into groups, yielding C_x-α, C_y-α and C_y / C_x-α graphs shown in figure 5. These graphs are used for analyzing the differences in the hydrodynamic properties of the four otter-board models.

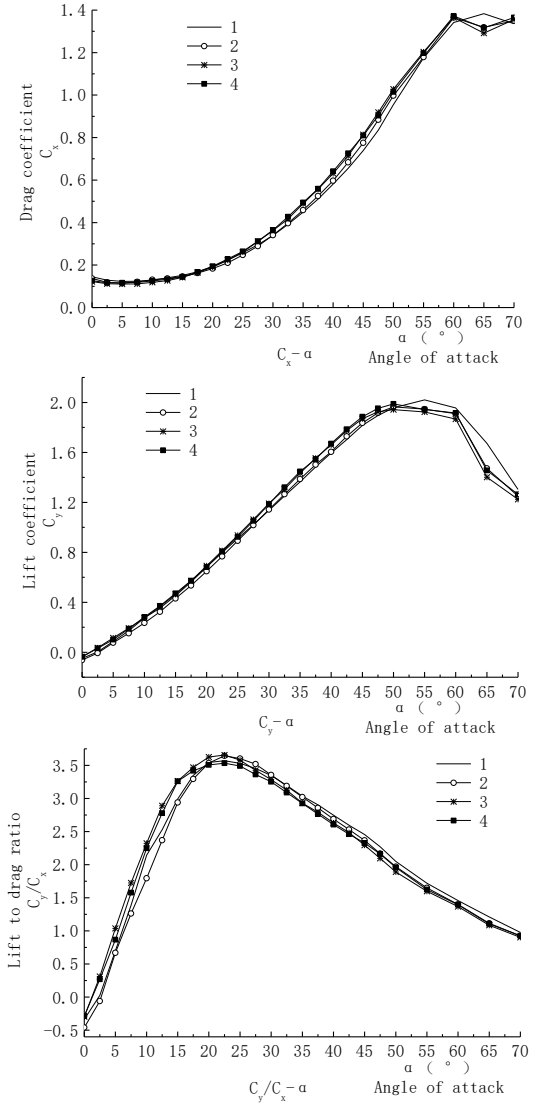

Fig. 5. Hydrodynamic properties of four otter-board models across a range of angle of attack.

In figure 5, C_x-α and C_y-α graphs show the variation curve of the drag and lift coefficient of the four models while the angle of attack α changes. The maximum lift coefficients C_y of No. 1, No. 2, No. 3, and No. 4 otter-board models were 2.020 (α = 55°), 1.965 (α = 50 °), 1.942 (α = 50 °), and 1.988 (α = 50 °), respectively. It shows that the maximum lift coefficient of No.1 model with the deflector curvature 0.06 is largest.

3.2 Lift-drag ratio

In figure 5, the maximum lift–drag ratios of No.3 model with the deflector curvature 0.12, there is 3.655 (α = 22.5 °). The maximum lift–drag ratios of No. 1, No. 2 and No. 4 models are 3.571 (α = 22.5 °), 3.644 (α = 22.5 °) and 3.534 (α = 22.5°), respectively. The higher or lower curvature of defectors may result in a lower maximum lift–drag ratio.

3.3 Stability of otter-board

Pitching moment can be divided into upper and lower pitching moments, which are usually distinguished by positive and negative values, Positive means the otter-board tilts backward, and negative means tilts forward. Its absolute value represents the level of pitching moment; and the pitching moment coefficient tending to 0 represents the more excellent stability of otter-board. In practice, comparing the absolute value C_m corresponding to the operation angle of attack of otter-board may determine the stability level of otter-board. For comparison, the angle of attack corresponding to the maximum lift–drag ratio C_y/C_x is selected [20]. The corresponding absolute value of C_m is shown in table 2. The absolute value of C_m of No. 3 model is 0.144, so hence, the stability of No. 3 otter-board model is better in pitch.

Table 2. Parameters of four otter-board models for stability analysis.

No.	Angle corresponding to the maximum lift –drag ratio α	$\lvert C_m \rvert$	Variable coefficient of C_p
1	22.5°	0.183	6.83%
2	22.5°	0.163	7.85%
3	22.5°	0.144	8.13%
4	22.5°	0.160	7.81%

The stability in roll of otter-board can be measured according to the center of pressure coefficient C_p; and the way of comparison is analyzing the coefficient of variation in C_p within the range of angle approximately 5° of the angle of attack corresponding to the maximum lift–drag ratio; a smaller coefficient results in the improved stability [21]. The calculated data are shown in table 2. The minimum variation coefficient of C_p is 6.83%; this value also means that the stability of No. 1 otter-board model is better in roll of otter-board.

4 Conclusion

Test analysis shows that the curvature of two deflectors has a point for equilibrating the hydrodynamic performances of otter-board. No.3 otter-board with the deflector curvature of 0.12 has the higher maximum lift–drag ratio at the angle of attack 22.5°, and at this angle of attack, the lift coefficient (0.813) is also higher than the other three models. In the meanwhile, the stability of No.3 otter-board model in pitch is also better comparatively, and the stability of No.1 otter-board model in roll is better. The data and conclusions of this study can provide a reference for the design of otter-board.

Acknowledgements

This work is financially supported by the National Key Technology R&D Program (No. 2013BAD13B04).

References

1. G. X. Guo, T. Y. Liu, X. H. Huang, F. L. Gu. Theory and Practice of trawl doors Kinetic. Guang. Sci. & Tech. Pub. (2008)
2. Y. Q. Zhou. Mechanics of fishing gear. Chi. Agr. Pub. (2001)
3. X. Z. Chen, X. C. Huang. Theory and method of gear model test. Sh. Sci. & Tech. Pub. (2011)
4. A. Sala, J. Prat, J. Antonijuan, A. Lucchetti. Fis. Res. **156**, 100(2009)
5. Y. Takahashi, Y. Fujimori, F. X. Hu, X. L. Shen, N. Kimura. Fis. Res. **400**, 161(2015)
6. M. K. Broadhurst, D. J. Sterling, R. B. Millar. Fis. Man. & Eco. **407**, 22(2015)
7. K. Fukuda, F. X. Hu, T. Tokai, K. Matuda. Ni. Su. Gak. **97**, 66(2000)
8. C. D. Park, K. Matuda, F. X. Hu. Ni. Su. Gak. **920**, 62(1996)
9. X. L. Shen, F. X. Hu, T. Kumazawa, D. Shiode, T. Tokai. Fis. Sci. **433**, 81(2015)
10. L. Wang, L. M. Wang, C. L. Feng, A. Z. Zhou, W. W. Yu, Y. Zhang, X. Zhang. Aqu. & Fis. **234**, 2(2017)
11. L. Wang, L. M. Wang, J. G. Shi, Y. Zhang, Y. L. Liu, W. W. Yu, X. Zhang. MAT. W. Con. **5004**, 128(2017)
12. L. Wang, L. M. Wang, A. Z. Zhou, J. G. Shi, Y. Zhang, G. D. Xu, X. Zhang. MAT. W. Con. **5003**, 128(2017)
13. L. Wang, L. M. Wang, C. L. Feng, X. Zhang, A. Z. Zhou, Y. Zhang, Y. L. Liu, G. R. Qi. Mar. Fis. **682**, 39(2017)
14. X. Zhang, J. H. Wang, M. Y. Wang, Y. F. Yu, B. S. Xu. Jou. Fis. Sci. Ch. **5**, 11(2004)
15. J. H. Wang, M. Y. Wang, X. Zhang, Y. F. Yu, B. S. Xu. Jou. Fis. Sci. Ch. **9**, S1(2004)
16. M. Y. Wang, J. H. Wang, X. Zhang, Y. F. Yu, B. S. Xu. Jou. Fis. Ch. **311**, 3(2004)
17. C. C. Li, Z. L. Liang, L. Y. Huang, W. F. Zhou, P. Sun, L. Wang. Mar. Sci. **69**, 11(2013)
18. L. Wang, L. M. Wang, C. L. Feng, X. Zhang, J. G. Shi, Y. Zhang, Y. L. Liu, W. W. Yu. Fis. Mod. **55**, 6(2015)

19. L. Wang, L. M. Wang, W. W. Yu, C. L. Feng, J. G. Shi, Y. L. Liu, X. Zhang. Con. In. For. En. Sus. De. **530**, 75(2016)
20. L. Yang. Fis. Sci. Tec. **38**, 2(1996)
21. L. Yang. Fis. Sci. Tec. **42**, 5(1996)